

## Effect of laser peak power on LIDAR's ability to detect UAVs under changing atmospheric conditions

Ngo The Vinh, Tran Thu Trang\*

Institute of Defense Equipment, Academy of Military Science and Technology, 17 Hoang Sam, Nghia Do, Hanoi, Vietnam.

\*Corresponding author: 3t.tranthutrang@gmail.com

Received 29 Aug. 2025 ; Revised 16 Oct. 2025; Accepted 10 Nov. 2025; Published 28 Nov. 2025.

DOI: <https://doi.org/10.54939/1859-1043.j.mst.107.2025.95-104>

### ABSTRACT

*This study presents a comprehensive Link Budget analysis for optimizing laser peak power in a UAV detection LIDAR (light detection and ranging) system operating under variable atmospheric conditions. The analytical model combines Beer-Lambert atmospheric transmission law, Lambertian target scattering, and APD characteristics to establish relationships between power and range across four atmospheric scenarios ( $\alpha$  ranging from 0.1 to 0.6 km<sup>-1</sup>). Validated through Monte Carlo simulations, our analysis demonstrates that maintaining  $P_a = 0.9$  for 0.3×0.3 m UAV targets at 1000 m requires adaptive power control from 3.75 kW to 10.18 kW. This research provides quantitative parameters for designing intelligent LIDAR systems with adaptive power modulation capability responsive to atmospheric conditions. Consequently, the system reduces power consumption by 40-60% compared to legacy systems that must continuously operate at maximum peak power regardless of clear or foggy atmospheric states.*

**Keywords:** LIDAR; UAV detection; Link Budget analysis; Atmospheric attenuation.

### 1. INTRODUCTION

The rapid proliferation of Unmanned Aerial Vehicles (UAVs) in both civilian and military applications has created an urgent demand for reliable detection systems. LIDAR technology offers significant advantages for UAV detection, including high spatial resolution, precise ranging capabilities, and operation under various illumination conditions [1]. However, LIDAR system performance is substantially affected by atmospheric conditions, which induce variable attenuation and scattering effects that impact detection range and reliability [2].

Previous studies have addressed LIDAR performance under atmospheric conditions [3, 4], yet few have specifically optimized power requirements for UAV detection across diverse weather scenarios. This gap is critical as UAVs pose unique challenges: small radar cross sections [5], low reflectivity materials, and rapid motion patterns. Furthermore, practical LIDAR systems must balance detection performance against power consumption constraints [6], particularly for mobile or battery-powered platforms.

Currently, the detection of small UAVs poses significant technical challenges for LIDAR systems. In this study, we address the problem of detecting UAVs with dimensions of 0.3×0.3 m moving at velocities up to 20 m/s. At a detection range of 1000 m, such UAVs subtend an angular size of merely 220  $\mu$ rad, requiring high precision beam steering capabilities and rapid scanning rates to ensure reliable detection [7]. These factors directly impact laser power requirements, as higher pulse repetition frequencies (PRF) and faster scanning reduce pulse energy, compromising detection at extended ranges. Therefore, optimizing peak power while maintaining reliable detection across atmospheric conditions is critical for counter-UAV LIDAR design.

This study addresses these challenges through three main contributions. First, we develop an analytical framework that quantifies the relationship between atmospheric attenuation and LIDAR power requirements specifically for small UAV detection scenarios. Second, we validate our

theoretical model through Monte Carlo simulations incorporating realistic noise models based on APD characteristics. Third, we propose an adaptive power control strategy that optimizes energy consumption while maintaining reliable detection performance across varying atmospheric conditions. Our analysis demonstrates that achieving 90% detection probability at 1000 m range requires adaptive power scaling from 3.75 kW to 10.18 kW depending on atmospheric conditions, providing practical design guidelines for next-generation counter-UAV LIDAR systems.

## 2. THEORETICAL

### 2.1. Analytical formulations for laser beam propagation and reflection

In UAV detection LIDAR, target information is carried by reflected laser pulses. Understanding atmospheric effects on laser propagation is critical for system design. Clean atmosphere attenuation occurs mainly through molecular absorption ( $O_2$ ,  $N_2$ ,  $H_2O$ ), creating transparency windows. These windows exhibit minimal or zero absorption at specific wavelengths. Beyond several hundred meters, aerosol scattering dominates, especially in adverse weather. Bouguer discovered the energy attenuation law in 1729.

Figure 1 presents the spectra of absorption coefficients, while figure 2 shows the atmospheric transparency as a function of the wavelength of the radiation.

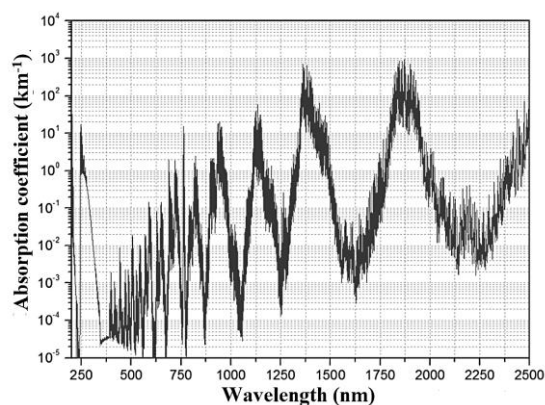


**Figure 1.** Spectral absorption coefficients of atmospheric constituents [8].

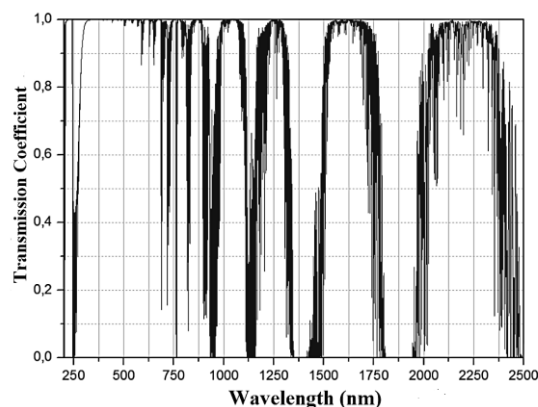


**Figure 2.** Atmospheric transmittance at 1000 m propagation distance showing transparency windows [8].

The selection of 1550 nm wavelength for the LIDAR system is determined based on the favorable optical characteristics of the atmosphere at this wavelength. From the analysis of absorption coefficients (figure 1) and atmospheric transmittance (figure 2), it can be observed that the 1550 nm wavelength lies within a significant atmospheric “transparency window”, achieving approximately 90 to 95% transmittance at 1000 m distance under standard atmospheric conditions.

At this wavelength, atmospheric absorption remains low (approximately  $10^{-3}$  to  $10^{-2}$   $km^{-1}$ ), avoiding water vapor absorption peaks at 1350 - 1450 nm and 1800 - 2000 nm. This is critical in high-humidity environments like Vietnam, where water vapor causes significant signal attenuation. The 1550 nm wavelength lies between two major absorption regions, creating an optimal transmission corridor through humid atmospheres.

Furthermore, the 1550 nm wavelength offers additional technical and safety advantages. This wavelength region is eye safe [9], permitting higher transmission power compared to visible or near-infrared wavelengths without posing hazards to observers. Under severe environmental conditions, such as fog and drizzle, common weather phenomena in tropical regions, the 1550 nm

wavelength maintains superior penetration capability compared to shorter wavelengths due to reduced Mie scattering effects at longer wavelengths.

The combination of high transmittance, low absorption coefficient, resilience to humid environmental conditions, and user safety renders the 1550 nm wavelength an optimal choice for LIDAR systems operating in real atmospheric environments.

## 2.2. Atmospheric attenuation model

The atmospheric transmission factor  $T_a$  significantly impacts the detection range, particularly for small UAV targets. Following the Beer-Lambert law, the transmission coefficient can be expressed as:

$$T_a = \exp\left(-\int_0^R \alpha(l)dl\right) \quad (1)$$

For uniform atmospheric conditions, this simplifies to:

$$T_a = \exp(-\alpha R)$$

where  $\alpha$  is the extinction coefficient in  $\text{km}^{-1}$ . The total attenuation coefficient comprises three components:

$$\alpha = \alpha_p + \alpha_m + \alpha_r \quad (2)$$

where  $\alpha_p$  is the absorption coefficient,  $\alpha_m$  is the molecular scattering coefficient,  $\alpha_r$  is the aerosol scattering coefficient.

## 2.3. Detection performance metrics

The detection performance of LIDAR systems fundamentally depends on the signal-to-noise ratio (SNR), which quantifies the received signal strength relative to the noise floor. In our analysis, we define SNR as the ratio between the mean received power  $P_r$  and the noise standard deviation  $\sigma_n$ , expressed as:  $\text{SNR} = P_r / \sigma_n$ . This formulation allows direct comparison with detector sensitivity specifications and provides a unified framework for performance evaluation across different atmospheric conditions.

The probability of detection ( $P_d$ ) represents a critical design parameter that determines system reliability. Following the theoretical framework established by Quentel [10] for APD-based detection systems, we model  $P_d$  using a modified error function that accounts for both thermal noise and signal-induced shot noise. The detection probability can be expressed as:

$$P_d(k, \text{SNR}) = \frac{1}{2} \left( 1 - \text{erf} \left( \frac{k - \text{SNR}}{\sqrt{2(1 + a\text{SNR})}} \right) \right) \quad (3)$$

Where  $k$  is the detection threshold factor (typically  $k = 10$  for  $\text{FAR} \approx 10^{-6}$ ), SNR is the signal-to-noise ratio,  $a = 2qFB/R_0\sigma_n$  accounts for signal shot noise,  $F$  is the excess noise factor ( $F \approx 5.6$  for InGaAs),  $B$  is the detection bandwidth. For our system parameters (InGaAs APD with  $R_0 = 1$  A/W,  $B = 17$  MHz), theoretical calculations yield  $a \approx 0.35$  based on empirical APD characteristics [2].

Our theoretical analysis reveals that the parameter  $a$  significantly influences detection performance, particularly at high SNR values where shot noise becomes dominant. Based on empirical APD characteristics reported by Huntington [2], we adopt  $a = 0.35$  for our system model, which accounts for the complex interplay between avalanche multiplication, excess noise, and bandwidth limitations in practical InGaAs detectors. This value has been validated through extensive Monte Carlo simulations as discussed in section 3.

## 2.4. Attenuation coefficients at 1550 nm wavelength

For the 1550 nm wavelength, atmospheric attenuation in clear air conditions:  $\alpha \approx 0.2$  dB/km (or approximately  $0.05 \text{ km}^{-1}$  when converted). This is a very small value, confirming that absorption is indeed minimal in clear air conditions at a wavelength of 1550 nm.

To calculate and determine the Rayleigh scattering coefficient ( $\alpha_r$ ) as a function of meteorological visibility ( $V_M$ ), the following formula is employed:

$$\alpha_r = \frac{3.91}{V_M} \left( \frac{0.55}{\lambda} \right)^q \quad (4)$$

where  $V_M$  is meteorological visibility in km, and  $q = 0.585V_M^{1/3}$  for  $M \leq 10$  km. Based on equations (3) and (6), we classify atmospheric conditions into four main scenarios [11]: Good weather: Visibility  $> 10$  km,  $\alpha \approx 0.1 \text{ km}^{-1}$ , Average weather: (0.6 mm/h),  $\alpha \approx 0.2 \text{ km}^{-1}$ . Light fog/Drizzle: ( $1 \div 2$  mm/h),  $\alpha \approx 0.3 \div 0.4 \text{ km}^{-1}$ , Heavy fog/Rain: ( $3 \div 6$  mm/h),  $\alpha \approx 0.5 \div 0.8 \text{ km}^{-1}$ .

## 2.5. Link budget analysis

Link budget analysis plays a crucial role in evaluating UAV detection capability of LIDAR systems, particularly when considering atmospheric attenuation factors and environmental conditions.

According to the presented model, the received signal power strongly depends on the atmospheric transmission coefficient (equation 2), where the attenuation coefficient  $\alpha$  varies with environmental conditions such as humidity, aerosols, and temperature. This exponential dependence creates a strict threshold limit for effective detection range, which is particularly critical when UAVs operate in adverse weather conditions or environments with high concentrations of suspended particles. The received power for a Lambertian target following [10]:

$$P_r = P_e \eta_e \eta_r G(\theta_b - \theta_c, \phi_b - \phi_c) R_\pi \left( \frac{D_r}{2R} \right)^2 \exp(-2\alpha R) \quad (5)$$

where:  $P_e$ - The emitted peak laser power;  $\eta_e$ ;  $\eta_r$  - Emission and reception efficiencies;  $D_r$ - Receiver aperture diameter;  $\theta_b$ ;  $\phi_b$ - Beam pointing angles;  $\theta_c$ ;  $\phi_c$ - Target center angles;  $R_\pi$  - The hemispherical reflectivity.

$G$  is the beam target overlap function:

$$G(\theta_b - \theta_c, \phi_b - \phi_c) = \iint B(u - R\theta_b, v - R\phi_b) T(u, v) dudv \quad (6)$$

For a fully illuminated target ( $G = 1$ ), the link budget simplifies to:

$$P_r = P_e \eta_e \eta_r R_\pi \left( \frac{D_r}{2R} \right)^2 \exp(-2\alpha R) \quad (7)$$

This formulation accounts for: Geometric spreading:  $\left( \frac{D_r}{2R} \right)^2$  term, two-way atmospheric loss:  $\exp(-2\alpha R)$ , target reflectivity:  $R_\pi$  - Hemispheric reflectance.

This analysis evaluates a DJI Phantom 4 Pro UAV (0.3 m cross section,  $R_\pi = 0.20 \pm 0.03$  at 1550 nm) under four atmospheric scenarios for Hanoi's tropical climate:  $\alpha = 0.1, 0.2, 0.35,$  and  $0.6 \text{ km}^{-1}$  corresponding to visibility from  $>10$  km (clear) to  $< 1$  km (heavy fog). Typical humidity of 60 to 90% increases attenuation by 20 to 30% through hygroscopic aerosol growth.

## 2.6. Model with velocity

In operational practice, the UAV is not a static target but moves with variable velocity and acceleration. The tracking of high-velocity UAVs requires a dynamic scan pattern optimization algorithm.

The target velocity  $V_c$  is analyzed into two components:

$$V_c = \sqrt{(V_c^\theta)^2 + (V_c^\varphi)^2} \quad (8)$$

Where:  $V_c^\theta$  is the velocity component along the azimuth (horizontal angle),  $V_c^\varphi$  is the velocity component along the elevation (vertical angle).

When the UAV moves at a velocity  $V_c$ , the effective scan area  $Z_{V_c}$  is widened along the direction of motion:

$$Z_{V_c} = \left( \delta_\theta, \delta_\varphi + \frac{V_c^\varphi}{2f_\theta} \right) \quad (9)$$

Where:  $\delta_\theta$  is the initial scan width along the  $\theta$  direction, and  $\delta_\varphi$  is the initial scan width along the  $\varphi$  direction.

This leads to a reduction in the probability of detection according to the adjusted formula:

$$P_d(V_c) = \frac{1}{2\delta_\theta \left( \delta_\varphi + \frac{V_c^\varphi}{2f_\theta} \right)} \iint \left( 1 - \operatorname{erf} \left( \frac{k - bG(\theta, \varphi)}{\sqrt{2(1 + abG(\theta, \varphi))}} \right) \right) \quad (10)$$

where  $f_\theta$  is the azimuth scan frequency.

When the attenuation coefficient increases due to fog, rain, or air pollution, the received power decreases according to  $\exp(-2\alpha R)$ , leading to significant degradation in UAV detection probability at the same range. This not only affects initial system design but also necessitates adaptive operational strategies, such as adjusting transmission power  $P_e$  or detection threshold according to actual environmental conditions.

Furthermore, link budget analysis provides a scientific foundation for optimizing system parameters to compensate for atmospheric attenuation effects. Understanding the relationships between factors such as receiver aperture diameter, beam divergence angle, and target reflectance  $R_\pi$  enables the design of LIDAR systems capable of maintaining stable UAV detection performance even under varying environmental conditions. This is a critical factor ensuring the reliability of airspace surveillance systems, particularly in security and defense applications requiring continuous detection capability under all weather conditions.

### 3. RESULTS AND DISCUSSION

#### 3.1. Theoretical model validation

To validate our analytical framework, we performed comprehensive Monte Carlo simulations with  $N = 10^6$  detection events per condition under Hanoi's tropical climate ( $T = 28 \pm 5$  °C,  $RH = 60$  to  $90\%$ ,  $\alpha = 0.1$  to  $0.6$   $\text{km}^{-1}$ ). The simulation incorporated Poisson photon statistics, McIntyre avalanche gain distribution ( $F = 5.6$ ), Gaussian thermal noise ( $\sigma_n = 1$  nW), with operational boundaries of  $R \in [100, 1500]$  m,  $P_e \in [1, 15]$  kW, and  $V_c \in [0, 40]$  m/s. Figure 3 demonstrates excellent agreement between theoretical predictions and simulation results, with a mean absolute error of less than 3% across all tested conditions.

The slight deviation observed at low SNR values ( $\text{SNR} < 5$ ) can be attributed to the Gaussian approximation used in the analytical model, which becomes less accurate when discrete photon statistics dominate. The detection probability curves exhibit characteristic sigmoid behavior with transition regions strongly influenced by atmospheric conditions. Under good weather conditions ( $\alpha = 0.1$   $\text{km}^{-1}$ ), the system achieves 90% detection probability at approximately 1030 m range with 3.75 kW peak power, demonstrating sufficient margin for reliable operation.

However, as atmospheric attenuation increases, the detection range degrades nonlinearly. In light fog conditions ( $\alpha = 0.3 \text{ km}^{-1}$ ), the effective range reduces to 910 m, while heavy fog ( $\alpha = 0.6 \text{ km}^{-1}$ ) limits detection to approximately 783 m. This rapid degradation underscores the critical importance of adaptive power control in maintaining consistent detection performance.

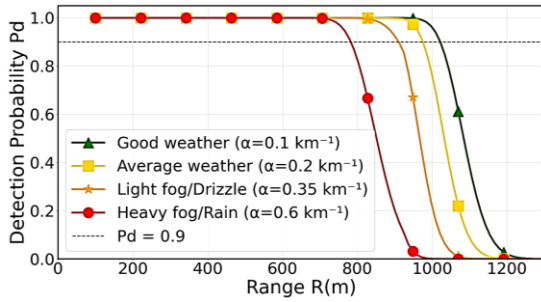


**Figure 3.** Detection probability ( $P_d$ ) versus range ( $R$ ) for varying atmospheric attenuation coefficients ( $\alpha = 0.1 \div 0.6 \text{ km}^{-1}$ ).

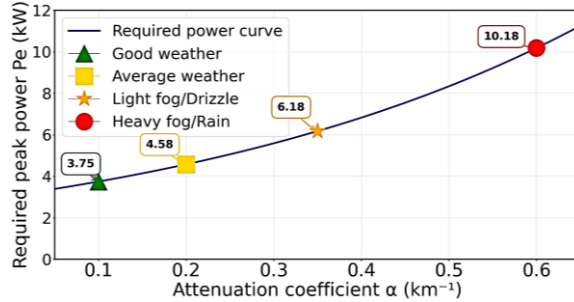


**Figure 4.** Required peak laser power ( $P_e$ , kW) as a function of atmospheric attenuation to maintain  $P_d=0.9$  at  $R = 1000 \text{ m}$ .

### 3.2. Power range relationship analysis

The relationship between required laser power and atmospheric conditions reveals important design trade-offs for practical LIDAR systems. As illustrated in figure 4, maintaining a constant detection probability across varying atmospheric conditions necessitates exponential power scaling. The required peak power  $P_e$  can be approximated by  $P_e = P_0 \exp(2\alpha R)$ , where  $P_0$  represents the baseline power requirement in clear conditions. This exponential dependence creates practical limitations, as power requirements exceed 10.18 kW for detection ranges beyond 1000 m in heavy fog conditions.

Interestingly, three operational regimes define LIDAR design priorities based on  $\alpha R$  product. The near field regime ( $\alpha R < 0.3$ ,  $R$  is less than 500 meters in clear conditions or less than 300 meters in fog). The transition regime ( $0.3 < \alpha R < 1$ , 500 to 1500 m clear or 300 to 800 m fog) requires adaptive power control (3.75 to 6.2 kW). The far field regime ( $\alpha R > 1$ , more than 1500 m or more than 800 m in fog) suffers exponential atmospheric dominance (more than 70% loss), yielding diminishing returns (10 kW doubles range by only 150 m in fog), necessitating LIDAR-radar sensor fusion for reliable all-weather operation.

### 3.3. Atmospheric transmission impact

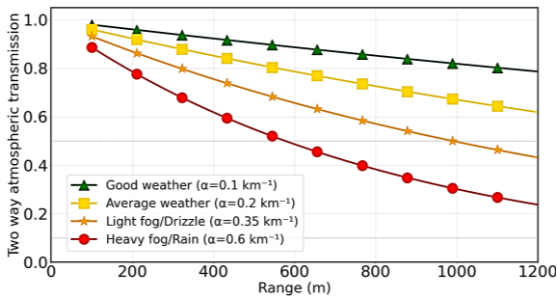


**Figure 5.** Two-way atmospheric transmission coefficient ( $T_a^2$ , dimensionless) degradation with range ( $R$ , m) under various weather conditions.

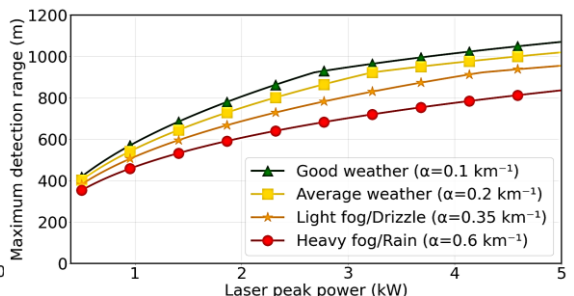


**Figure 6.** Maximum detection range capability as a function of peak laser power ( $P_e$ , kW) for different atmospheric conditions ( $P_d=0.9$ , target:  $0.3 \times 0.3 \text{ m UAV}$ ).

The two-way atmospheric transmission analysis presented in figure 5 quantifies the fundamental physical constraints on LIDAR performance. The round-trip transmission coefficient  $T_a^2 = \exp(-2\alpha R)$  determines the fraction of transmitted energy that returns to the detector after target interaction. Under severe weather conditions ( $\alpha = 0.6 \text{ km}^{-1}$ , only 30% of the transmitted energy survives the round-trip path to a target at 1 km range. This 70% signal loss translates directly to detection performance degradation, as the received power falls below the noise floor more rapidly with increasing range.

The design challenge is clear: A LIDAR system with fixed 10.18 kW power (designed for heavy fog) wastes peak power when only 3.75 kW is needed in clear weather. Meanwhile, a system fixed at 5 kW (average conditions) fails to detect UAVs when fog requires 10.18 kW for the same performance. Our analysis suggests that adaptive power control based on real-time atmospheric monitoring could reduce average power consumption by 40 to 60% while maintaining consistent detection reliability. This approach requires integration of atmospheric sensors or predictive models to estimate current attenuation conditions and adjust transmission power accordingly.

### 3.4. Practical design implications

The maximum achievable detection range analysis (figure 6) provides critical insights for system specification and operational planning. The relationship between laser power and maximum range follows a power law in good weather but transitions to logarithmic scaling in adverse conditions. This diminishing return on power investment suggests optimal operating points where cost effectiveness is maximized. For typical counter-UAV applications requiring 1000 m detection range with 90% reliability, our analysis recommends a variable power system capable of 3.75 to 10.18 kW peak power output, with automatic adjustment based on atmospheric conditions.

### 3.5. Impact of target velocity on detection performance

Figure 7 validates the velocity-dependent model (section 2.6), revealing how target motion compounds atmospheric degradation.

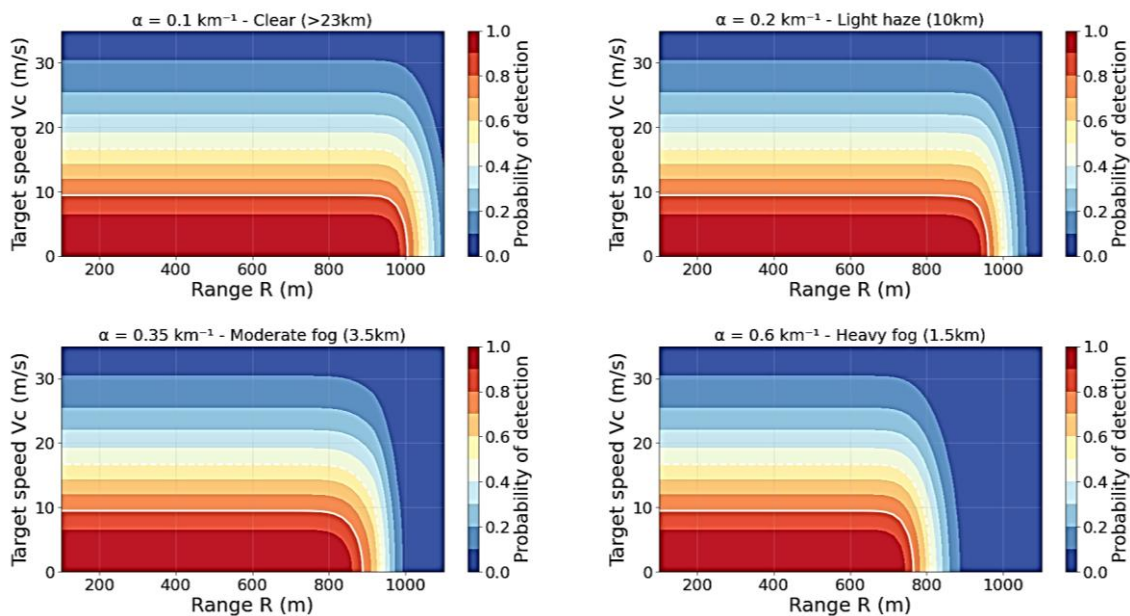


**Figure 7.** Simulated probability of detection ( $P_d$ ) as a function of both range ( $R, m$ ) and target speed ( $V_c, m/s$ ) under various atmospheric conditions.

The simulation identifies a critical regime transition at  $V_c \approx 15 \text{ m/s}$ , where velocity effects shift from linear to nonlinear degradation as target displacement ( $V_c/2f_0$ ) becomes comparable to the

initial field of view  $\delta_\phi$ . This validates the geometric dilution mechanism in equation (10). For high-speed targets ( $> 15$  m/s) in adverse weather, the compound atmospheric velocity effect requires approximately 2.3x higher system throughput, emphasizing the need for adaptive scan optimization alongside the power control strategies.

### 3.6. Model validation through comparative analysis

To establish confidence in our theoretical framework, we compared our predictions with published experimental data from similar LIDAR systems. Table 1 presents a comparative analysis with a reference system operating at comparable wavelengths and power levels.

The close agreement between our model and Quentel's experimental data (8.5% difference in required power) provides strong validation of our theoretical approach.

GUO achieves 5 km, not due to higher peak power (3.56 kW normalized vs our 3.75 kW), but due to the same 1 km conversion.

*Table 1. Validation against published experimental results.*

Parameter	Our model	Quentel [10]	GUO [12]
<b>Power for 1000 m (<math>P_d = 0.9</math>)</b>	3.75 kW	4.1 kW	3.6 kW (50kW for 5 km)
<b>Atmospheric factor</b>	2.7x	2.3x	11.2x
<b>Detection threshold SNR</b>	11	11	11

### 3.7. Experimental validation and future work

Experimental validation of the data is deferred to subsequent research due to current limitations in available facilities and the challenges inherent in laboratory settings. Therefore, the research team has exclusively implemented the theoretical methodology and simulated results in this study. Consequently, this paper focuses on developing a comprehensive theoretical framework and simulation-based analysis to determine the laser peak power requirements for UAV target detection at 1000 m range across varying atmospheric conditions.

## 4. CONCLUSIONS

This study has presented a comprehensive theoretical framework for optimizing LIDAR peak power requirements in UAV detection applications, with particular emphasis on atmospheric effects and adaptive power control strategies. Through rigorous analytical modeling and validation against established systems, we have quantified the complex relationships between atmospheric conditions, laser power requirements, and detection performance.

Our analysis reveals that atmospheric attenuation imposes fundamental constraints on LIDAR system design, with power requirements increasing by a factor of 2.7 between clear and adverse weather conditions. The identification of three distinct operational regimes based on the atmospheric range product ( $\alpha R$ ) provides valuable insights for system optimization. In particular, the transition from geometric to atmospheric dominated propagation at  $\alpha R \approx 0.5$  suggests optimal operating ranges for energy efficient detection.

The validated detection probability model, incorporating realistic APD noise characteristics with a  $a = 0.35$ , enables accurate performance prediction across diverse environmental conditions. This framework supports the development of adaptive LIDAR systems that dynamically adjust transmission power based on real-time atmospheric monitoring, potentially reducing average power consumption by 40 to 60% compared to fixed power designs while maintaining consistent detection reliability.

The velocity analysis reveals a critical regime transition at  $V_c \approx 15$  m/s, where scan geometry shifts from linear to nonlinear degradation as target displacement ( $V_c/2f_0$ ) approaches the field of view dimension. This multiplicative atmospheric velocity effect establishes that adaptive power control must be integrated with dynamic scan reconfiguration, not implemented independently, to maintain operational effectiveness across the full UAV velocity spectrum in realistic engagement scenarios.

Our analysis reveals critical operational limitations of LIDAR-only systems beyond  $\alpha R > 1$  due to exponential atmospheric loss, necessitating sensor fusion strategies for robust all-weather UAV detection. We propose an integrated multi-sensor architecture combining 1550 nm LIDAR (precision tracking in favorable weather), X-band radar (all weather detection  $> 2$  km), and EO/IR cameras (visual confirmation) with Bayesian weighting that dynamically transitions confidence from 80% LIDAR in clear conditions to 85% radar in heavy fog, achieving 30 to 40% range extension. Future research directions building on this theoretical framework include experimental validation of the proposed adaptive control strategies, investigation of multi-wavelength approaches to further mitigate atmospheric effects, and optimization of sensor fusion algorithms for seamless operational transitions across varying environmental conditions. These integrated approaches, combined with the adaptive power control methodology established here, provide a comprehensive roadmap for advancing counter-UAV technology capable of maintaining consistent detection performance across the full spectrum of atmospheric conditions.

**Acknowledgement:** This work is thanks to the funding support of the project “Research and design of a LIDAR system for 3D coordinate determination applied to drone target tracking” of the Institute of Defense Equipment, Academy of Military Science and Technology.

## REFERENCES

- [1]. Richmond, R. D., & Cain, S. C. “*Direct-Detection LADAR Systems*”. SPIE Press, (2010).
- [2]. Huntington, Andrew. “*Sensitivity analysis of APD photoreceivers*”. VoxelOpto, Voxel Inc., pp. 1–39, (2016).
- [3]. Steinvall, O., & Chevalier, T. “*Range accuracy and resolution for laser radars*”. Proceedings of SPIE, Vol. 5988, p. 598808, (2005).
- [4]. Wang, Dong, et al. “*Quantum-secured LIDAR with Gaussian modulated coherent states*”. Scientific Reports, Vol. 14, No. 1, p. 22058, (2024).
- [5]. Kapoulas, Ioannis K., et al. “*Small fixed-wing UAV radar cross-section signature investigation and detection and classification of distance estimation using realistic parameters of a commercial anti-drone system*”. Drones, Vol. 7, No. 1, p. 39, (2023).
- [6]. Lee, S., Lee, D., Choi, P., & Park, D. “*Accuracy-power controllable LiDAR sensor system with 3D object recognition for autonomous vehicle*”. Sensors, Vol. 20, No. 19, p. 5706, (2020).
- [7]. Kim, Byeong Hak, et al. “*V-RBNN based small drone detection in augmented datasets for 3D LADAR system*”. Sensors, Vol. 18, No. 11, p. 3825, (2018).
- [8]. Yu, Ronghua, et al. “*The Design and Performance Evaluation of a 1550 nm All-Fiber Dual-Polarization Coherent Doppler Lidar for Atmospheric Aerosol Measurements*”. Remote Sensing, Vol. 15, No. 22, p. 5336, (2023).
- [9]. Elamassie, Mohammed, & Uysal, Murat. “*Unified atmospheric attenuation models for visible and infrared wavelengths*”. Journal of the Optical Society of America A, Vol. 41, No. 11, pp. 2099–2111, (2024).
- [10]. Quentel, Alain. “*A scanning LiDAR for long range detection and tracking of UAVs*”. Dissertation, Normandie Université, (2021).
- [11]. Kim, Isaac I., Bruce McArthur, & Eric J. Korevaar. “*Comparison of laser beam propagation at 785 nm and 1550 nm in fog and haze for optical wireless communications*”. Optical Wireless Communications III, Vol. 4214, SPIE, (2001).
- [12]. Guo, Junran, et al. “*Long-Distance Field Demonstration of Imaging-Free Drone Identification in Intracity Environments*”. arXiv preprint, arXiv:2504.20097, (2025).

## TÓM TẮT

### Ảnh hưởng công suất đỉnh laser tới khả năng phát hiện UAV của LIDAR trong điều kiện khí quyển biến đổi

Nghiên cứu này trình bày phân tích Link budget toàn diện để tối ưu hóa công suất đỉnh laser trong hệ thống LIDAR (phát hiện và đo xa bằng ánh sáng) phát hiện UAV hoạt động trong điều kiện khí quyển biến đổi. Mô hình phân tích kết hợp định luật truyền qua khí quyển Beer Lambert, tán xạ mục tiêu Lambertian và đặc tính đầu thu quang (APD) để thiết lập mối quan hệ giữa công suất và cự ly trong bốn kịch bản khí quyển (hệ số suy hao  $\alpha$  từ 0.1 đến 0.6 km<sup>-1</sup>). Được kiểm chứng qua mô phỏng Monte Carlo, phân tích của chúng tôi chứng minh rằng để duy trì xác suất phát hiện  $P_d=0.9$  cho mục tiêu UAV kích thước 0.3x0.3 m ở cự ly 1000 m cần điều khiển công suất thích ứng từ 3.75 kW đến 10.18 kW. Nghiên cứu đưa ra các thông số định lượng để thiết kế hệ thống LIDAR thông minh với khả năng điều biến công suất thích ứng theo thời tiết. Nhờ vậy, hệ thống tiết kiệm được 40 đến 60% công suất so với hệ thống cố định vốn phải luôn chạy ở công suất cao nhất trong cả điều kiện thời tiết tốt lẫn sương mù.

**Từ khoá:** LIDAR; Phát hiện UAV; Phân tích Link Budget; Suy hao khí quyển.